OpenDM Damage Model Theory Manual

Bryce Mazurowski

November 15, 2024

1 Problem Definition

1.1 Solid mechanics: infinitesimal deformation

The partial differential equation we wish to solve is the balance of linear momentum. Stated in strong form neglecting inertial effects and body forces:

$$\nabla \cdot \boldsymbol{\sigma} = 0 \quad \forall \boldsymbol{x} \in \Omega \tag{1}$$

with boundary conditions

$$\begin{aligned} \boldsymbol{u} &= \bar{\boldsymbol{u}} \quad \forall \boldsymbol{x} \in \Gamma_d \\ \boldsymbol{\sigma} \cdot \boldsymbol{n} &= \bar{\boldsymbol{t}} \quad \forall \boldsymbol{x} \in \Gamma_n \end{aligned} \tag{2}$$

The relationship between stress and strain is

$$\boldsymbol{\sigma} = \bar{\boldsymbol{C}} : \boldsymbol{\varepsilon} \tag{3}$$

The infinitesimal strain tensor is used

$$\boldsymbol{\varepsilon} = \frac{1}{2}(\nabla \boldsymbol{u} + \nabla^T \boldsymbol{u})$$

where $\boldsymbol{u}$ is the displacement solution to the problem.

1.2 Weak Form

The method of weighted residuals is used to arrive at the weak form of the problem:

$$\int_\Omega \nabla \boldsymbol{w} : \boldsymbol{\sigma}(\boldsymbol{u}) d\Omega = \int_{\Gamma_n} \boldsymbol{w} \cdot \bar{\boldsymbol{t}} d\Gamma \tag{4}$$

where $\boldsymbol{w} \in H^1$ is an arbitrary weight function and $\boldsymbol{u} \in H^1$ is the displacement solution.

1.3 Material nonlinearity:

Material nonlinearity requires a special solver. Newton-Raphson is the classical choice. However, as discussed in Section 2.3.1, for the OpenDM Damage Models a Quasi-Newton solver is used. This is because the material tangent stiffness matrix is not exact. The displacement solution becomes incremental:

$$\boldsymbol{u}_n = \sum_{j=0}^{n} \Delta \boldsymbol{u}_j$$

With updates at each NR solve at each load step:

$$\boldsymbol{u}_{n+1} = \boldsymbol{u}_n + \Delta \boldsymbol{u}_{n+1}$$

The weak form can be used to define a residual:

$$R = \int_{\Gamma_n} \boldsymbol{w} \cdot \bar{\boldsymbol{t}} d\Gamma - \int_{\Omega} \nabla \boldsymbol{w} : \boldsymbol{\sigma}(\boldsymbol{u}) d\Omega$$

Then the residual is linearized via a Taylor Series:

$$R(\boldsymbol{u}_{n+1}) = R(\boldsymbol{u}_n) + \frac{\partial R}{\partial \boldsymbol{u}}(\boldsymbol{u}_n)\delta \boldsymbol{u}_{n+1} + O(\delta \boldsymbol{u}^2)$$

Progressing from a converged solution, $R(\boldsymbol{u}_n) = 0$, dropping higher order terms:

$$\frac{\partial R}{\partial \boldsymbol{u}}(\boldsymbol{u}_n)\delta \boldsymbol{u}_{n+1} \approx R(\boldsymbol{u}_{n+1})$$

The quantity $\boldsymbol{u}_{n+1}$ is found iteratively in the Newton-Raphson scheme. So we solve a given load step n for a number of NR increments i as:

$$\frac{\partial R}{\partial \boldsymbol{u}}(\boldsymbol{u}_n^i)\delta \boldsymbol{u}_{n+1}^{i+1} = R(\boldsymbol{u}_n^i)$$

With our residual, this becomes:

$$\int_{\Omega} \nabla \boldsymbol{w} : \frac{\partial \boldsymbol{\sigma}}{\partial \boldsymbol{u}} \delta \boldsymbol{u}_{n+1}^{i+1} d\Omega = \int_{\Gamma_n} \boldsymbol{w} \cdot \bar{\boldsymbol{t}}^{n+1} d\Omega - \int_{\Omega} \nabla \boldsymbol{w} : \boldsymbol{\sigma}(\boldsymbol{u}_n^i) d\Omega$$

Once the system of equations is solved for a given i, the displacement is updated. The residual is then recomputed, and can be used as a convergence check. The term $\frac{\partial \boldsymbol{\sigma}}{\partial \boldsymbol{u}}$ is the material tangent stiffness matrix. This matrix is computed based on the formulation of the OpenDM material model.

2 OpenDM Damage Models

OpenDM damage models are based on the formulation in the papers (1, 4). These works are based on the Onera formulation in (2, 3).

To simplify presentation of the models, stresses and strains are given in Voigt notation, that is:

$$\begin{aligned} \boldsymbol{\varepsilon} &= [\varepsilon_{11}, \varepsilon_{22}, \varepsilon_{33}, 2\varepsilon_{23}, 2\varepsilon_{13}, 2\varepsilon_{12}]^T = [\varepsilon_1, \varepsilon_2, \varepsilon_3, \varepsilon_4, \varepsilon_5, \varepsilon_6]^T \\ \boldsymbol{\sigma} &= [\sigma_{11}, \sigma_{22}, \sigma_{33}, \sigma_{23}, \sigma_{13}, \sigma_{12}]^T = [\sigma_1, \sigma_2, \sigma_3, \sigma_4, \sigma_5, \sigma_6]^T \end{aligned} \tag{5}$$

All quantities are also given in material coordinates $\hat{\boldsymbol{x}}$.

The Helmholtz Free Energy is defined as

$$\psi = \frac{1}{2\rho}(\boldsymbol{\varepsilon}^* \cdot \bar{\boldsymbol{C}} \boldsymbol{\varepsilon}^*), \tag{6}$$

where ρ is density, $\boldsymbol{\varepsilon}^*$ is the mechanical strain, and $\bar{\boldsymbol{C}}$ effective material stiffness.

For now, thermal strain $\boldsymbol{\varepsilon}^{th}$ is taken to always be zero, this is an area ripe for future work. Material stress behavior is then the derivative of the Helmholtz free energy with respect to the strain,

$$\boldsymbol{\sigma} = \bar{\boldsymbol{C}} \boldsymbol{\varepsilon}^*. \tag{7}$$

The material stiffness tensor is defined as

$$\bar{\boldsymbol{C}} = (\bar{\boldsymbol{S}})^{-1}, \tag{8}$$

where $\bar{\boldsymbol{S}}$ is the effective material compliance tensor. The definition of $\bar{\boldsymbol{S}}$ is where the damage modes begin to appear

$$\bar{\boldsymbol{S}} = \boldsymbol{S}^0 + \sum_{n=1}^{2} d^n \boldsymbol{H}^n, \tag{9}$$

where $\boldsymbol{S}^0$ is the undamaged material stiffness tensor and d^n is the damage variable for mode $n = 1, 2, 4, 5$ with the final two removed in the 2-Mode model. $\boldsymbol{H}^n, n = 1, 2, 4, 5$ are constants that modify material compliance these tensors are defined for their respective damage model below. The 2-Mode model makes use of $\boldsymbol{H}^1$ and $\boldsymbol{H}^2$ only.

Energy dissipation as a result of matrix microcracking is captured by independent dissipation potentials for each damage mode. Each mode has the same form,

$$F^n = f(y^n) - d^n. \tag{10}$$

The driving forces y^n vary for each mode and model and are defined below.The definition of $f(y^n)$ is carried out over two steps, first

$$g^n = \frac{\langle \sqrt{y^n_{max}} - \sqrt{y^n_0} \rangle_+}{\sqrt{y^n_c}}, \tag{11}$$

where y^n_{max} adds a history effect to the model, which takes the largest y^n value over time for each mode calculation at a given material point and $\langle \cdot \rangle_+$ is the positive Macaulay bracket. Model parameter y^n_0 sets a threshold value of the driving force to start damage. Another parameter y^n_c changes the celerity of the damage progression. Then, the definition of $f(y^n)$ is

$$f(y^n) = d^n_c[1 - \exp(-(g^n)^{(p^n)})]. \tag{12}$$

An additional parameter d^n_c sets the maximum value that a given damage mode can reach and a final parameter p^n changes the shape of the curve of damage progression.

2.1 2-Mode Model

Matrix microcracking perpendicular to each fiber direction is captured by the 2-Mode model. Matrix microcrack growth for each mode is shown in Figure 1.

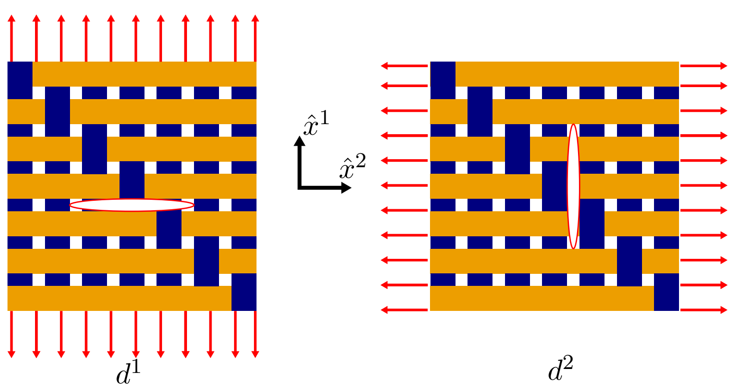

Figure 1: Damage modes in material coordinates $\hat{\boldsymbol{x}}$ for the OpenDM 2-Mode damage model. Representative matrix microcracks are shown for each damage mode.

The definition of $\boldsymbol{H}^1$ and $\boldsymbol{H}^2$ is

$$\boldsymbol{H}^1 = \begin{bmatrix} \eta^1 h^1_1 S^0_{11} & 0 & 0 & 0 & 0 & 0 \\ 0 & 0 & 0 & 0 & 0 & 0 \\ 0 & 0 & 0 & 0 & 0 & 0 \\ 0 & 0 & 0 & 0 & 0 & 0 \\ 0 & 0 & 0 & 0 & h^1_3 S^0_{55} & 0 \\ 0 & 0 & 0 & 0 & 0 & h^1_2 S^0_{66} \end{bmatrix}, \ \boldsymbol{H}^2 = \begin{bmatrix} 0 & 0 & 0 & 0 & 0 & 0 \\ 0 & \eta^2 h^2_1 S_{22} & 0 & 0 & 0 & 0 \\ 0 & 0 & 0 & 0 & 0 & 0 \\ 0 & 0 & 0 & h^2_3 S_{44} & 0 & 0 \\ 0 & 0 & 0 & 0 & 0 & 0 \\ 0 & 0 & 0 & 0 & 0 & h^2_2 S_{66} \end{bmatrix}, \tag{13}$$

where h^n_1, h^n_2, and h^n_3 are model parameters that scale the effect of each fracture mode on material compliance for damage mode n. The nonzero parts of $\boldsymbol{H}^n$ represent effect of Mode I, II, III microcrack growth associated with each mode. Microcrack closure is captured by the function η^n for each mode n. In (3), a progressive deactivation rule is used to represent microcracks closing at different times. Here a simple on-off function based on the current strain is used

$$\eta^n = \begin{cases} 1 & \boldsymbol{\varepsilon}^n \geq 0 \\ 0 & else \end{cases}, \tag{14}$$

where $\boldsymbol{\varepsilon}^n$ is the normal strain associated with Mode I fracture for each damage mode. In Equation (13), there is only damage deactivation for Mode I. This is consistent with closed cracks, as shear stresses (Mode II and III) can still affect the stiffness under compressive normal loads.

The driving forces for modes 1 and 2 are then

$$\begin{aligned} y^1 &= \frac{1}{2}(\varepsilon_1^+ C_{11}^0 \varepsilon_1^+ + b_2 \varepsilon_5 C_{55}^0 \varepsilon_5 + b_1 \varepsilon_6 C_{66}^0 \varepsilon_6), \\ y^2 &= \frac{1}{2}(\varepsilon_2^+ C_{22}^0 \varepsilon_2^+ + b_2 \varepsilon_4 C_{44}^0 \varepsilon_4 + b_1 \varepsilon_6 C_{66}^0 \varepsilon_6), \end{aligned} \tag{15}$$

where $\boldsymbol{C}^0$ is the undamaged stiffness tensor and $b_i, i = 1, 2$, are mode-specific shear coupling parameters that increase the effect shear strains have on damage growth.

The quantities ε_1^+ and ε_2^+ indicate the positive part of the normal strain. A Macaulay bracket is used to calculate this for each strain component. This assures that compressive normal force does not contribute to the driving force for either damage mode, which is consistent with microcrack closure.

2.2 4-Mode Model

In the 4-mode model, the first two damage modes represent the same type of microcracking as in the previous model. The additional two capture matrix microcracks that are oriented 45° in either direction from the fiber direction. The four damage modes are shown in Figure 2.

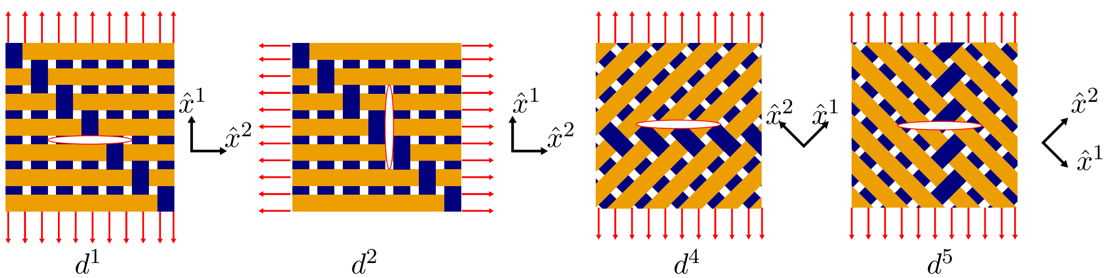

Figure 2: Damage modes in material coordinates $\hat{\boldsymbol{x}}$ for the OpenDM 4-Mode damage model. Representative matrix microcracks are shown for each damage mode.

The definition of $\boldsymbol{H}^1$ and $\boldsymbol{H}^2$ from Equation (13) are used again. For d^4 and d^5, a new definition is given. Since this damage is not aligned with the material coordinates, the compliance tensor is not orthotropic, but anisotropic. A rotated compliance tensor $\bar{\boldsymbol{S}}$ is used, transformed either by a 45° rotation about the $\hat{\boldsymbol{x}}_3$ axis for d^4 or a $-45°$ rotation about the $\hat{\boldsymbol{x}}_3$ axis for d^5. The tensors $\bar{\boldsymbol{H}}^n, n = 4, 5$ is defined in the respective coordinate system as

$$\bar{\boldsymbol{H}}^n = \begin{bmatrix} \eta^n h_1^n \bar{S}_{11}^0 & 0 & 0 & 0 & h_4^n \bar{S}_{15}^0 & h_4^n \bar{S}_{16}^0 \\ 0 & 0 & 0 & 0 & 0 & 0 \\ 0 & 0 & 0 & 0 & 0 & 0 \\ 0 & 0 & 0 & 0 & 0 & 0 \\ h_4^n \bar{S}_{15}^0 & 0 & 0 & 0 & h_3^n \bar{S}_{55}^0 & 0 \\ h_4^n \bar{S}_{16}^0 & 0 & 0 & 0 & 0 & h_2^n \bar{S}_{66}^0 \end{bmatrix}, \tag{16}$$

where $\bar{\boldsymbol{S}}^0$ is the undamaged compliance tensor in damage coordinates. $\bar{\boldsymbol{H}}^n$ needs to be transformed back to material coordinates before use. With a proper transformation matrix $\boldsymbol{T}^n$ for the corresponding damage mode coordinate system, $\boldsymbol{H}^n, n = 4, 5$ is defined as

$$\boldsymbol{H}^n = \boldsymbol{T}^{\boldsymbol{S},n} \bar{\boldsymbol{H}}^n (\boldsymbol{T}^{\boldsymbol{S},n})^T \tag{17}$$

where h_1^n, h_2^n, h_3^n, and h_4^n are model parameters that scale the effect of each fracture mode on material compliance for damage mode n and $\boldsymbol{T}^{\boldsymbol{S},n}$ is the transformation from the compliance tensor that transforms from the damage coordiantes to material coordinates. The additional parameter h_4^n, which captures the now nonzero contribution to Mode II and III fracture from the rotated compliance tensor. The $\boldsymbol{H}^n$ matrices represent the same effects as in the 2-Mode model, that is increased compliance from Mode I, II, and III fracture. Equation (14) is again used to capture microcrack closure for each mode. In the d^4 and d^5 case, the normal strain in the rotated coordinates are used to turn the damage on or off.

The driving forces for this model are considerably more complicated. They are defined in two steps, the first is a strain energy type quantity

$$
\begin{aligned}
z_1 &= \frac{1}{2}(\varepsilon_1^{d^{1+}} \boldsymbol{C}_{11}^0 \varepsilon_1^{d^{1+}} + b_2 \varepsilon_5^{d^{1+}} \boldsymbol{C}_{55}^0 \varepsilon_5^{d^{1+}} + b_1 \varepsilon_6^{d^{1+}} \boldsymbol{C}_{66}^0 \varepsilon_6^{d^{1+}}), \\
z_2 &= \frac{1}{2}(\varepsilon_2^{d^{2+}} \boldsymbol{C}_{11}^0 \varepsilon_1^{d^{2+}} + b_2 \varepsilon_4^{d^{2+}} \boldsymbol{C}_{44}^0 \varepsilon_4^{d^{2+}} + b_1 \varepsilon_6^{d^{2+}} \boldsymbol{C}_{66}^0 \varepsilon_6^{d^{2+}}), \\
z_6 &= \frac{1}{4}(\varepsilon_1^{d^{1+}} \boldsymbol{C}_{11}^0 \varepsilon_6^{d^{1+}} + \varepsilon_2^{d^{2+}} \boldsymbol{C}_{22}^0 \varepsilon_6^{d^{2+}} + b_3 \boldsymbol{C}_{66}^0 (\varepsilon_6^{d^{1+}} \varepsilon_1^{d^{1+}} + \varepsilon_6^{d^{2+}} \varepsilon_2^{d^{2+}}),
\end{aligned}
\tag{18}
$$

where $\boldsymbol{\varepsilon}^{d^{1+}}$ and $\boldsymbol{\varepsilon}^{d^{2+}}$ are the positive parts of the strain tensor for the d^1 and d^2 modes, and b_3 is an additional parameter to control the effect of shear coupling in driving damage. Each mode's strain decomposition is

$$
\begin{aligned}
\boldsymbol{\varepsilon}^{d^1} &= [\varepsilon_1, 0, 0, \varepsilon_5, \varepsilon_6]^T \\
\boldsymbol{\varepsilon}^{d^2} &= [0, \varepsilon_2, 0, \varepsilon_4, 0, \varepsilon_6]^T.
\end{aligned}
\tag{19}
$$

A Macaulay bracket on the eigenvalues of the strain is used to compute the positive part of the strain, as discussed in (5). The calculation is as follows

$$
\varepsilon_i^+ = P_{ij} \langle \hat{\varepsilon_j} \rangle_+, \tag{20}
$$

where $\hat{\boldsymbol{\varepsilon}}$ is the vector of eigenvalues of the strain tensor and $\boldsymbol{P}$ is the projection tensor that transforms strain from the spectral basis to the material basis.

The driving forces used in Equation (10) are then

$$
\begin{aligned}
y^1 &= z_1 - |z_6| \\
y^2 &= z_2 - |z_6| \\
y^4 &= \langle z_6 \rangle_+ \\
y^5 &= \langle z_6 \rangle_-
\end{aligned}
\tag{21}
$$

2.3 Tangent Stiffness Tensor

For both the 2-Mode and 4-Mode models, the numerical tangent stiffness tensor is used. The analytical tangent is certainly tractable for the 2-Mode model, but the 4-Mode model is quite complicated. In the 4-Mode model, behavior depends on the eigenvalues, which requires a transformation. The transformation matrix then depends on the eigenvectors. To simplify this process, the numerical tangent is used.

The numerical tangent is based on a Taylor series approximation of the stress field

$$
\sigma_i(\boldsymbol{\varepsilon} + \delta\varepsilon_j) = \sigma_i(\boldsymbol{\varepsilon}) + \frac{\partial \sigma_i}{\partial \varepsilon_j}(\boldsymbol{\varepsilon})(\delta\varepsilon_j) + O(\delta\varepsilon_j^2), \tag{22}
$$

where there is a bit of notation abuse in $\boldsymbol{\varepsilon} + \delta\varepsilon_j$, which is meant to represent the current strain perturbed in the \$j\$-th component by a magnitude of $\delta\varepsilon$.

Equation~(22) is then rearranged to get the tangent stiffness tensor $\boldsymbol{C}^{tan}$

$$
\boldsymbol{C}_{ij}^{tan} = \frac{\partial \sigma_i}{\partial \varepsilon_j} = \frac{\sigma_i(\boldsymbol{\varepsilon} + \delta\varepsilon_j) - \sigma_i(\boldsymbol{\varepsilon})}{\delta\varepsilon}. \tag{23}
$$

In words, for each perturbation of strain the difference in stress response is calculated, and then normalized by the magnitude of the perturbation. Each strain perturbation corresponds to a column of the tangent stiffness tensor.

Both the 2-Mode and 4-Mode tangent tensor can be nonsymmetric. This is quite cumbersome to deal with numerically, in terms of solver time and memory, so the tangent is symmetrized

$$\hat{\boldsymbol{C}}^{tan} = \frac{1}{2}(\boldsymbol{C}^{tan} + (\boldsymbol{C}^{tan})^T). \tag{24}$$

This does mean that the tangent stiffness tensor is not exact, and thus a Newton-Raphson solver becomes a quasi-newton solver. Also, this generally has some effect on the convergence of the system, but the symmetrized tensor likely makes up for this with a quicker and less memory-dense solver.

2.3.1 General comments about the tangent stiffness matrix

Both the 2-Mode and 4-Mode tangent tensor can be nonsymmetric. This is quite cumbersome to deal with numerically, in terms of solver time and memory, so the tangent is symmetrized

$$\hat{\boldsymbol{C}}^{tan} = \frac{1}{2}(\boldsymbol{C}^{tan} + (\boldsymbol{C}^{tan})^T). \tag{25}$$

This does mean that the tangent stiffness tensor is not exact, and thus a Newton-Raphson solver becomes a quasi-newton solver. Also, this generally has some effect on the convergence of the system, but the symmetrized tensor likely makes up for this with a quicker and less memory-dense solver.

In the numerical explorations of the 2-Mode and 4-Mode damage models, both have exhibited softening. This occurs as a result of combined damage modes and manifests as negative eigenvalues in the tangent stiffness tensor. This has been more of a problem in the 4-Mode model, as is evidenced in Section~**??**. Several attempts to remedy this have been unsuccessful, including using the nonsymmetric tangent tensor, using an arclength solver, smaller load steps, and attempts to change convergence tolerances in Abaqus. This is not an issue if only a single damage mode is active at a time. It is an issue in the validation tests where the response is more complicated. To remedy this, problems should be constructed to be displacement-controlled.

3 References

[1] Craig Przybyla and Antoine Débarre and Jean-François Maire and Emmanuel Baranger and Frédéric Laurin, *Scaler nonlinear continuum damage models for ceramic matrix composites with and without in plane ply anisotropy at room temperature*, Journal of European Ceramic Society, 2025.

[2] J. L. Chaboche and J. F. Maire, *A new micromechanics based CDM model and its application to CMC's*, Aerospace Science and Technology, 2002.

[3] Lionel Marcin and Jean-Francois Maire and Nicolas Carrère and Eric Martin, *Development of a Macroscopic Damage Model for Woven Ceramic Matrix Composites*, International Journal of Damage Mechanics, 2011.

[4] Mazurowski, Bryce and Przybyla, Craig and C. Armando Duarte, *Multiscale analysis of open holes and fasteners in CMC structures with the Generalized Finite Element Method*, Composite Structures, Submitted.

[5] Murakami, Sumio, *Continuum damage mechanics: a continuum mechanics approach to the analysis of damage and fracture*, Springer Science & Business Media, 2012.